

High Performance Photodetectors of Individual InSe Single Crystalline Nanowire

Jian-Jun Wang, Fei-Fei Cao, Lang Jiang, Yu-Guo Guo,* Wen-Ping Hu,* and Li-Jun Wan*

Beijing National Laboratory for Molecular Sciences, Institute of Chemistry, Chinese Academy of Sciences, Beijing 100190, China

Received August 26, 2009; E-mail: wanlijun@iccas.ac.cn

Nanomaterials of metal selenide have attracted particular attention recently due to their fascinating physical, optical, thermal, and electrical properties for potential applications in nanoelectronics, energy conversion, nanophotonics, and thermoelectrics.^{1–5} For example, properties of indium selenide can be tuned by its compositions, structures, and phases, so that optimal optical and electric devices can be achieved.^{5–7} Simultaneously, indium selenide can be used as a binary source for preparing diverse ternary derivatives such as CuInSe_2 ,^{8,9} and AgInSe_2 ,¹⁰ which are also promising candidates for optoelectronic devices. Pioneer works in this field include the growth of In_2Se_3 nanowires,^{5,11} phase control for crystal shape evolution of InSe nanostructures,⁷ the study of phase-change memory¹² of In_2Se_3 nanostructures, etc. However, to our knowledge, few reports have addressed the optical properties of InSe nanowires.

Photodetectors are key important elements of optoelectronics because the devices have higher sensitivity and lower noise, which combined are advantageous for light detection in a simple device.^{13–17} Therefore, the development of nanomaterials and the increasing demand for miniaturization and integration of optoelectronic devices all point to the cross-disciplinary role of high performance photodetectors of nanostructures. Herein we have synthesized InSe nanowires (NWs), and the new generated NWs are successfully applied to photodetectors. Reproducible, high-sensitivity photoresponse properties are demonstrated on individual InSe NWs.

InSe nanowires were synthesized *via* a physical vapor transport system in a horizontal tube furnace with In_2Se_3 as precursor.¹⁸ This method is a green method to yield highly pure nanomaterials without metal catalysts (see Supporting Information). Briefly, bulk In_2Se_3 was evaporated at the center of a horizontal tube furnace, and products were collected at downstream substrate. Figure 1a shows a typical scanning electron microscopy (SEM) image of as-grown InSe NWs, most of which exhibit a nanoribbon morphology. The InSe NWs have an average diameter ranging from 60 to 250 nm and a length up to tens of micrometers. Figure 1b is a representative transmission electron microscopy (TEM) image from a single NW, indicating a uniform diameter along their length. The chemical compositions of individual NWs were measured by energy dispersive X-ray spectroscopy (EDS) (Figure S1) which reveal the In/Se ratio is $\sim 1:1$.

The structures of InSe NWs were investigated by X-ray diffraction (XRD) and TEM. Figure 1c is the XRD pattern of the as-synthesized sample and clearly shows that the grown NWs are in a hexagonal structure with the lattice constants $a = 4.0 \text{ \AA}$ and $c = 16.6 \text{ \AA}$ (JCPDS-34-1431). Figure 1d is a high resolution (HR) TEM image of a single InSe NW showing a series of $(10\bar{1}0)$ planes with a spacing of 3.5 \AA , crossing each other at an angle of 60° . A selected area electron diffraction (SAED) pattern (Figure 1e) on a single NW shows well-defined diffraction patterns which confirms the

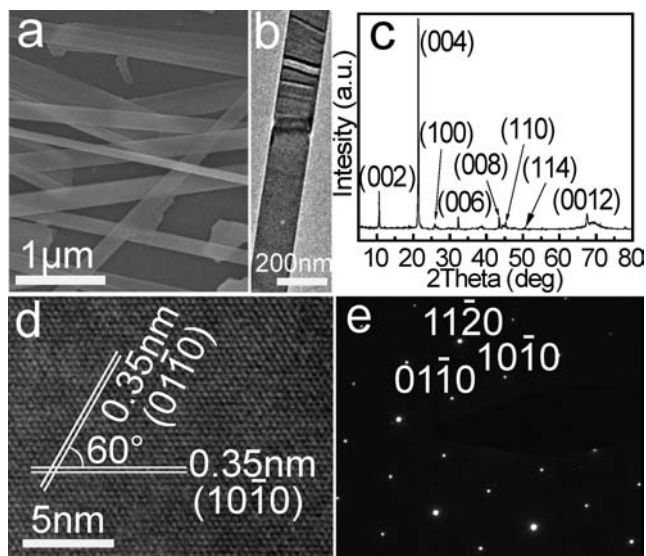


Figure 1. (a) SEM image of as-grown InSe NWs. (b) TEM image of a single NW. (c) XRD pattern of InSe NWs. (d) HRTEM image of a single InSe NW. (e) SAED pattern of a single InSe NW.

single crystalline nature of InSe NWs. The diffraction spots in the SAED pattern can be well indexed to hexagonal InSe.

The photoresponse characteristics of InSe NWs were investigated by fabricating a device based on a single NW. First, a single NW was transferred onto a Si/SiO₂ mechanically. Then, a copper grid covered the NW as a shield mask for electrode deposition. After the deposition the copper grid was removed. The schematic illustration of a single NW-based device is shown in Figure 2a. Current–voltage (I – V) characteristics of the devices were recorded with a Keithley 4200 SCS and a Micromanipulator 6150 probe station in a clean and shielded box at room temperature. An iodine–tungsten lamp was used as a white light source in view of the significant absorption of the as-grown InSe NWs in the wavelength range (see Figure S2). The single NW-based device exhibits excellent photoresponse characteristics as shown in Figure 2b. With the light irradiation on and off, the current of the devices shows two distinct states, a “low” current state under dark conditions and “high” current state under light conditions. The switching in those two states was reversible and fast, acting as a high quality photosensitive switch. At the “OFF” state, the current was only 40 pA. However, at the “ON” state, the current could approach 2000 pA, and the switching “ON/OFF” ratio is as high as 50. The high photosensitivity of the InSe NWs is further confirmed by photocurrent measurement in the devices based on a single InSe NW. The relationship between photocurrent and incident optical power densities, shown in Figure 2d, demonstrates a power dependence of ~ 0.67 , that is, $I \approx P^{0.67}$, indicating an excellent photocapture in the

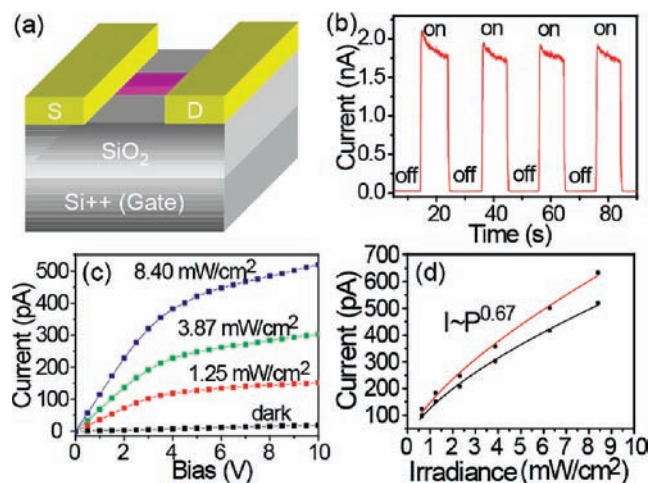


Figure 2. (a) Schematic illustration of a single NW-based device. (b) On-off switching of the single NW-based device at a power density of 8.40 mW cm^{-2} and a bias voltage of 40 V . (c) Dark current and photocurrents at different incident power densities. (d) Photocurrents measured versus incident optical densities at a bias voltage of 10 V (black) and 20 V (red). The corresponding functions are $I = 123.5 P^{0.67}$ and $I = 147.2 P^{0.67}$, respectively.

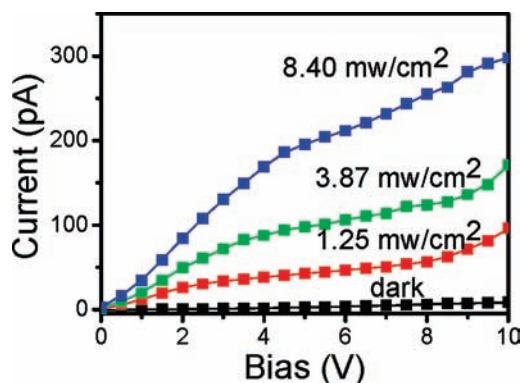


Figure 3. Dark current and photocurrents at different incident power densities of the device corresponding to Figure 3c after storing in air at room temperature for two months.

so-grown InSe NWs. These results show the prospective possibility of the InSe NWs as highly photosensitive detectors and a photo-switch. It should be noted that the on/off ratio of the devices exhibited an applied bias dependence, which was assigned to the applied bias dependence of the dissociation of excitons and the transport of the free carriers in the nanowire devices.

Finally, for practical application, the environmental stability of the photodetectors is a key parameter. The stability of the same single NW-based device in Figure 3 stored in air over two months was examined at room temperature. The results are shown in Figure

3 with almost the same results of photosensitivity as shown in Figure 2. The high photoresponse performance and environmental stability demonstrate the ability of a single InSe NW-based device in light detection and signal magnification for the development of low cost, ultrahigh density nanometer sized photoelectric integration.

In summary, a simple method was introduced to synthesize nanomaterials of a new metal selenide, InSe NWs. The photoresponse characteristics of InSe NWs were investigated by fabricating the devices based on a single NW. With the light irradiation on and off, the current of the device could respond at “high” and “low” states with the “ON/OFF” ratio as high as 50. Moreover, the high environmental stability of the so-prepared InSe NWs was demonstrated, indicating possible application for low cost, ultrahigh density nanometer sized photoelectric devices.

Acknowledgment. This work is supported by the National Natural Science Foundation of China (Grant Nos. 20603041, 20821003, 20733004, and 20701038), National Key Project on Basic Research (Grant Nos. 2006CB806100 and 2009CB930400), and the Chinese Academy of Sciences.

Supporting Information Available: The synthesis of the InSe NWs, the corresponding EDS, and the absorbance spectrum of the as-grown InSe NWs. This material is available free of charge via the Internet at <http://pubs.acs.org>.

References

- (1) Guo, Q.; Kim, S.; Kar, M.; Shafarman, W.; Birkmire, R.; Stach, E.; Agrawal, R.; Hillhouse, H. *Nano Lett.* **2008**, *8*, 2982–2987.
- (2) Jung, Y.; Lee, S.; Ko, D.; Agarwal, R. *J. Am. Chem. Soc.* **2006**, *128*, 14026–14027.
- (3) Luther, J.; Law, M.; Beard, M.; Song, Q.; Reese, M.; Ellingson, R.; Nozik, A. *Nano Lett.* **2008**, *8*, 3488–3492.
- (4) Panthani, M. G.; Akhavan, V.; Goodfellow, B.; Schmidtke, J. P.; Dunn, L.; Dodabalapur, A.; Barbara, P. F.; Korgel, B. A. *J. Am. Chem. Soc.* **2008**, *130*, 16770–16777.
- (5) Peng, H.; Xie, C.; Schoen, D.; Cui, Y. *Nano Lett.* **2008**, *8*, 1511–1516.
- (6) Tu, H.; Kelley, D. *Nano Lett.* **2006**, *6*, 116–122.
- (7) Park, K.; Jang, K.; Kim, S.; Kim, H.; Son, S. *J. Am. Chem. Soc.* **2006**, *128*, 14780–14781.
- (8) Schoen, D. T.; Peng, H. L.; Cui, Y. *J. Am. Chem. Soc.* **2009**, *131*, 7973–7975.
- (9) Yang, Y.; Chen, Y. *J. Phys. Chem. B* **2006**, *110*, 17370–17374.
- (10) Ng, M.; Boothroyd, C.; Vittal, J. *J. Am. Chem. Soc.* **2006**, *128*, 7118–7119.
- (11) Sun, X.; Yu, B.; Ng, G.; Nguyen, T.; Meyyappan, M. *Appl. Phys. Lett.* **2006**, *89*, 233121.
- (12) Yu, B.; Ju, S.; Sun, X.; Ng, G.; Nguyen, T.; Meyyappan, M.; Janes, D. *Appl. Phys. Lett.* **2007**, *91*, 133119.
- (13) Ettenberg, M. *Adv. Imaging* **2005**, *20*, 29–32.
- (14) Fossum, E. *IEEE Micro* **1998**, *18*, 8–15.
- (15) Kim, S.; Lim, Y. T.; Soltész, E. G.; De Grand, A. M.; Lee, J.; Nakayama, A.; Parker, J. A.; Mihaljevic, T.; Laurence, R. G.; Dor, D. M.; Cohn, L. H.; Bawendi, M. G.; Frangioni, J. V. *Nat. Biotechnol.* **2004**, *22*, 93–97.
- (16) Tang, J.; Konstantatos, G.; Hinds, S.; Myrskog, S.; Pattantyus-Abraham, A.; Clifford, J.; Sargent, E. *ACS Nano* **2008**, *3*, 331–338.
- (17) Wang, J.; Gudiksen, M.; Duan, X.; Cui, Y.; Lieber, C. *Science* **2001**, *293*, 1455–1457.
- (18) Zhang, Y.; Wang, N.; Gao, S.; He, R.; Miao, S.; Liu, J.; Zhu, J.; Zhang, X. *Chem. Mater.* **2002**, *14*, 3564–3568.

JA9072386